

**EXPERIMENTAL AND COMPUTATIONAL STUDIES OF FLUID  
FLOW PHENOMENA IN CARBON DIOXIDE SEQUESTRATION  
IN BRINE AND OIL FIELDS**

Chuang Ji ( [chuang.ji@netl.doe.gov](mailto:chuang.ji@netl.doe.gov) )  
National Energy Technology Laboratory  
Department of Energy, Morgantown, WV 26507-0880  
BOX 5725 Clarkson University  
Potsdam, NY 13699

Goodarz Ahmadi ( [ahmadi@clarkson.edu](mailto:ahmadi@clarkson.edu) )  
BOX 5725 Clarkson University  
Potsdam, NY 13699

Duane H. Smith ( [duane.smith@netl.doe.gov](mailto:duane.smith@netl.doe.gov) )  
National Energy Technology Laboratory  
Department of Energy, Morgantown, WV 26507-0880

## INTRODUCTION

Sequestration of CO<sub>2</sub> by injection into deep geological formations is a method to reduce CO<sub>2</sub> emissions into the atmosphere. However, when CO<sub>2</sub> is injected underground, it forms fingers extending into the rock pores saturated with brine or petroleum. This flow instability phenomenon, known as viscous fingering, is significant for CO<sub>2</sub> sequestration because it will govern the available volume for CO<sub>2</sub> storage in the deep formation. Thus a greater understanding of viscous fingering could ultimately lead to increased capacities for CO<sub>2</sub> sequestration.

In our study, an experimental method is developed for providing a fundamental understanding of geological sequestration (Ogunsola, et al., 2000). In this experiment, a flow cell, which is an artificial porous medium made by etching channels of random width into glass plates, is used to simulate the CO<sub>2</sub> displacement of brine inside the opaque rock pores. Since the flow cell is transparent, the viscous fingering can be observed during the gas displacement of water through the flowcell. Images of the flow can be recorded and used to analyze the flow patterns and calculate saturations of water and gas. The pressure drop through the flow cell can also be measured and the relative permeability can be calculated.

To provide predictions and an explanation of the experimental results, a numerical simulation of this experiment is also conducted with FLUENT<sup>TM</sup> (a computer code for fluid flow). Here a flow cell with square-lattice grids of square cross-section flow channels is studied numerically. The geometry of the flow cell and the width of the channels are close to those of the physical flow cell. The boundary conditions, such as the inlet flow rate and the outlet pressure are chosen to be similar to the experimental conditions. The VOF free surface model of FLUENT<sup>TM</sup> Code is used in the analysis. This model is appropriate for studying two or more immiscible fluids with or without surface tension (Fluent User Guide, 1994). In this study, the simulations are performed for different fluid viscosity ratios with zero surface tension. Therefore the analysis is applicable to miscible fluids and/or the cases that the surface tension between the two immiscible fluids is very small.

The advantage of the computational model is that it provides the magnitudes of pressure, velocity, saturation and other properties of the fluid phases at each grid of the flowcell. The data may then be used for evaluating the relative permeability of different phases in the flow cell. The study shows that the relative permeability is a strong function of saturation. Furthermore, the relative permeability also varies with the flow pattern and the viscosity ratio of the fluid phases.

## **OBJECTIVE**

The objective of this project is to improve the efficiency of CO<sub>2</sub> geological sequestration in oil fields and brine saturated fields, to provide a more accurate description of two-phase flow in sequestration, and to develop a better understanding of the displacement of oil or brine by CO<sub>2</sub>.

## **APPROACH**

In this project, first a laboratory experiment is conducted. A flow cell, which is an artificial transparent porous medium, is used in the experiment. Pressure and flow rate of injected gas and displaced water are measured. The images of viscous fingering in the flow cell are recorded and analyzed to obtain residual saturations of gas and relative permeabilities of water and gas. Variations of flow pattern and relative permeability with the fluid properties, such as viscosity and density, and injection conditions, such as gas flow rate, are studied.

A numerical simulation of the experiment is also conducted with the FLUENT<sup>TM</sup> computational code. The multiphase flow model for two immiscible fluids is used to simulate the experimental conditions in the flow cell. The numerical results are to be compared with the experimental results and those obtained from other numerical models, such as pore-level model of CO<sub>2</sub> sequestration in oil fields and brine fields (Bromhal, et al., 2001; Ferer, et al., 2001).

## PROJECT DESCRIPTION

### EXPERIMENTAL SECTION

The experimental flow system, which is shown in Figure 1, consists of a flow cell, which simulates the porous medium, a syringe pump, which provides a constant-volume-rate injection of gas into the flow cell, a pressure transducer for measuring the pressure drop across the flow cell, and a balance for measuring the mass of displaced liquid.

The flow cell is made by etching channels of random width into a glass plate and fusing a second, flat plate to it, thereby creating a network of enclosed channels connected to inlet and outlet manifolds. Two flow cells having different channel widths were used in this study: Cell #1, with channel width uniformly distributed from 175-575  $\mu\text{m}$ , and Cell #2, with channel widths from 260-1305  $\mu\text{m}$ .

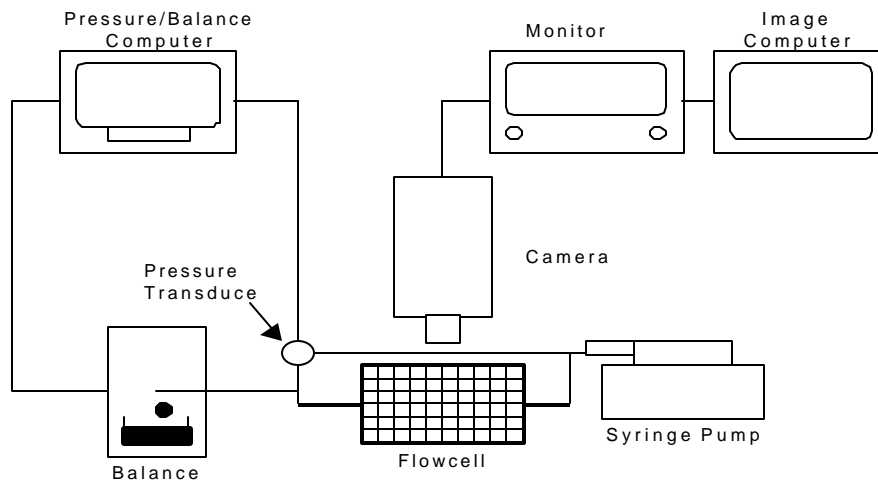


Figure 1. Experimental flow system

### COMPUTATIONAL SECTION

A computational model for the flow cell is developed, where a total of  $3 \times 206 \times 206$  grids were used. The square-lattice channels with an average width of 200 microns are distributed uniformly in the computational cell, with the top and bottom layers being sealed as boundaries. At the initial time the flow cell is flooded with fluid 1. Then fluid 2 is injected from

the inlet on the left side into the flow cell with a constant flow rate and the fluid 1 is displaced out of the flow cell from the outlet on the right hand side.

## RESULTS

This section presents results from experiments and numerical simulations with FLUENT<sup>TM</sup>. Pictures of the flow patterns in experimental and numerical simulations are shown, the phase permeabilities of fluid 1 and 2 are computed, and the relation between phase permeabilities and saturation is presented.

Figure 2 shows the flow pattern formed by injection of gas into a water-saturated cell. The flow cell is horizontal; and the cell inlet is on the left and the outlet is on the right. The air injection rate is roughly 0.5ml/min and the picture is taken at 10s after gas began to flow into the cell. In this figure, the bright area is occupied by gas and the water is in the dark area. It is seen that the gas penetrated into the flow cell and forms an irregular fractal interface with water.

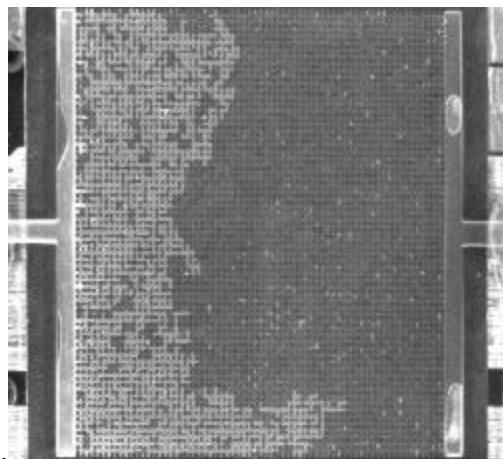


Figure 2. Picture of flow pattern in flow cell for a gas injection rate of 0.5ml/min at 10s.

Figure 3 shows a sample simulation result of the saturation condition in the flow cell after fluid 2 is injected into the flow cell for 10.5s. Here the viscosity ratio of fluid 1 to 2 is 58, the density ratio is 1000, and the surface tension is zero. The injection rate of fluid 2 is 0.5ml/min. In this figure, saturation of fluid 2 increases form 0 to 1 as the color of the channel

varies from dark blue to red. It is also seen that fluid 2 percolates into the flow cell with several fingers, some of which have penetrated across the flow cell.

It is also observed that an irregular interface between fluids 1 and 2 forms in the cell. The pattern shown in Figures 2 and 3 clearly illustrates the viscous fingering phenomenon that is observed in CO<sub>2</sub> sequestration.

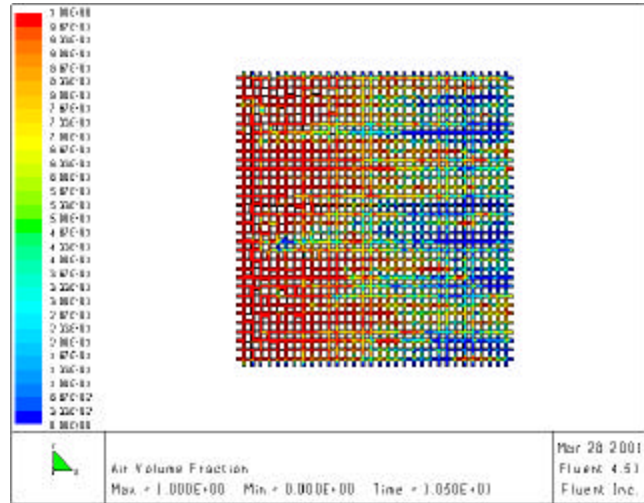


Figure 3. Variations of volume fraction of fluid 2 in the simulated flow cell.

To analyze the simulation data, a moving average method is used. Here a moving window of 206 × 16 grids is considered and moving averages across the flow cell are evaluated. Average saturation, pressure drop across the window, and velocities of fluid 1 and 2 in each block are computed. In Figure 4, the average saturation of fluid 1 and fluid 2 are shown for each block. Here the average saturation is evaluated using

$$S_n = \frac{\sum_{i=1}^{16} \sum_{j=1}^{206} s_{nij} l_{ij} w_{ij}}{\sum_{i=1}^{16} \sum_{j=1}^{206} l_{ij} w_{ij}} \quad (1)$$

where  $l_{ij}$  and  $w_{ij}$  are, respectively, the length and width of each grid, and  $S_n$  refers to the average saturation of fluid 1 or 2 at each block. In Equation (1) and in the subsequent analysis subscript  $n = 1$  or 2 corresponds to fluids 1 or 2, respectively.

Figure 4 shows that the average saturation of fluid 2 decreases gradually from the left side to the right side of the flow cell, while the saturation of fluid 1 increases

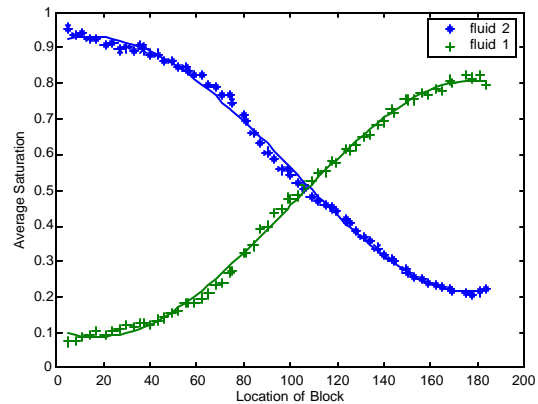


Figure 4. Average saturation of fluid 1 and 2 at each block.

with an opposite trend. Variations of computed saturation in Figure 4 are similar to those seen in Figure 3.

Similarly, the average velocities of fluid 1 and 2 across the cell are evaluated by a moving averaged defined as

$$V_n = \frac{\sum_{i=1}^{206} \sum_{j=1}^{206} f_{nij} S_{nij}}{\sum_{i=1}^{206} \sum_{j=1}^{206} l_{ij}} \quad (2)$$

where  $V_n$  refers to the average superficial velocity of fluid 1 or 2, and  $f_{nij}$  is the flow flux in the major flow direction of fluid 1 or 2 at each grid.

Figure 5 shows variations of the average superficial velocity across the cell. It is seen that average velocity of fluid 2 decreases from the inlet side toward the outlet, while the average velocity of fluid 1 increases as the outlet is approached.

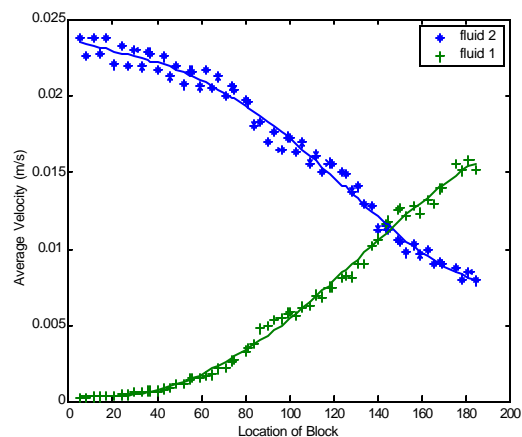


Figure 5. Average velocity of fluid 1 and 2 at each block.

To compute the pressure drop variations across the cell, first the average pressure at the inlet and outlet of each block are evaluated. That is

$$P_{im} = \frac{\sum_{j=1}^{206} P_{mj} l_{mj}}{\sum_{j=1}^{206} l_{mj}} \quad (3)$$

The pressure drop of each block is given by

$$P_i = P_{iI} - P_{iO} \quad (4)$$

where  $P_m$  refers to the average pressure at inlet or outlet of each block. Here  $m = I$  denotes inlet and  $m = O$  corresponds to outlet, and  $p_{im}$  is the pressure at each grid of inlet or outlet section of the moving average block.  $P_i$  is the pressure drop across each (moving average) block,

Figure 6 presents the pressure drop across each moving average block. It is seen that the pressure difference between the inlet and outlet of each block increases gradually across the flow cell.

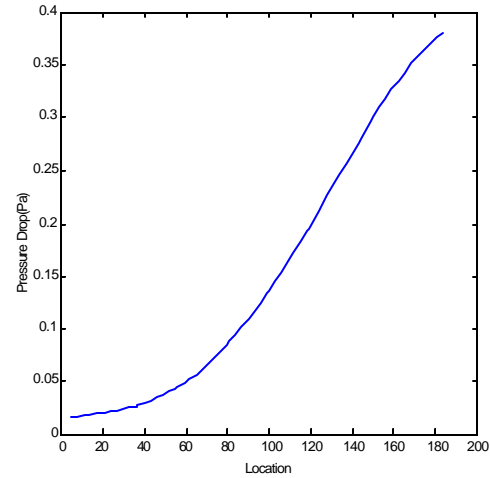


Figure 6. Pressure drop at each block.

According to Darcy's law, the phase permeabilities of fluid 1 and 2 are defined as

$$k_{ni} = \frac{V_i m_i}{P_i / L_i} \tag{5}$$

where  $k_n$  is the phase permeability,  $\eta_n$  is the viscosity and  $L_i$  is the width of each block. Plots of phase permeability of fluid 1 and 2 versus saturation of fluid 1 are presented in Figure 7. It is observed that the phase permeability of fluid 2 decreases sharply as the saturation of fluid 1 increases. This implies that in the parts of the cell that are mostly occupied by fluid 2, the relative permeability of fluid 1 is quite low. In contrast, the phase permeability of fluid 1 increases sharply its saturation increases.

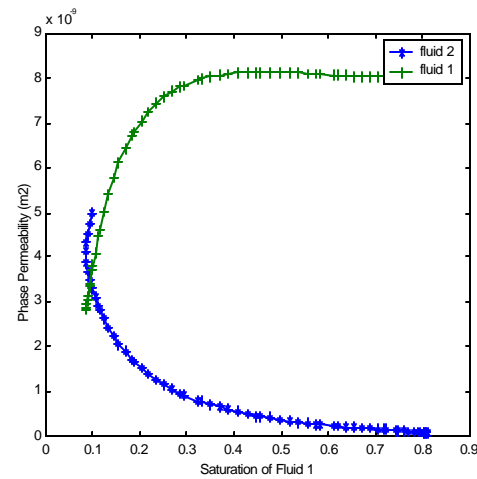


Figure 7. Permeabilities of fluid 1 and 2 for different saturation of fluid 1.

## **BENEFITS**

The present experimental approach provides a visible image of the flow pattern during the displacement of one fluid by another. The process can be observed and recorded to provide detailed information of the nature of multiphase flows in porous media. The laboratory data can then be used to test a variety of different computational models. The computational model also solves the exact dynamical equations for a viscous flow in small channels. Therefore, the model can accurately account for the viscous effects of the multiphase fluids flows in porous media. Extensions of the present study could also be used for assessing the limitations of the Darcy flow model for sequestration of CO<sub>2</sub> in formations saturated with oil and/or brine.

## **FUTURE ACTIVITIES**

The future experimental study includes the further development of experimental methods to improve the accuracy of measurement of pressure and flow rate. Another important aspect is to conduct the experiment with different orientations of the flow cell. The plan is to repeat the experiment with the flow cell set horizontally or vertically to measure the effect of gravity on the flow pattern.

Development of more detailed computer simulations is also an important part of the future study. We plan to study effects of the flow cell geometry and properties of different fluid phases, as well as injection conditions. We also plan to use the FLUENT<sup>TM</sup> code to develop a refined computational model of the flow cell and account for the surface tension and capillary effects as well as contact angle in addition to the viscous effects. The goal is to provide a better understanding of the effects flow patterns and residual saturation on the relative permeability under various conditions.

## REFERENCE

1. Bromhal, G.S., Ferer, M. and Smith, D.H., (2001) Pore-Level Modeling of Carbon Dioxide Sequestration in Oil Fields: A Study of viscous and Buoyancy Force , Proceedings of 1<sup>st</sup> National Conference on Carbon Sequestration, Washington, DC, May 14-17, 2001.
2. Ferer M., Bromhal, G.S. and Smith, D.H., (2001) Pore-Level Modeling of Carbon Dioxide Sequestration in Brine Fields, Proceedings of 1<sup>st</sup> National Conference on Carbon Sequestration, Washington, DC, May 14-17, 2001.
3. Fluent Users Guide, Version 4.52, Fluent Corp., Letanon, NH (1994)
4. Ogunsola, O., Ramer, E. and Smith, D.H., (2000) Analysis of Viscous Fingering in Two-Dimensional Flow Cell by Fractal Dimension, Fuel Division preprint, Washington, DC, August 20-24,2000.